

Erratum

Walker, J. A. and Westneat, M. W. (2002). Performance limits of labriform propulsion and correlates with fin shape and motion. *J. Exp. Biol.* **205**, 177–187.

In the printed version of this paper, the values for M2 and M3 in Table 1 were incorrect. The correct version of the table is given below and in the online version.

Table 1. *Fin shape data for four species of labrid fish*

	<i>Gomphosus</i>	<i>Halichoeres</i>	<i>Cirrhilabrus</i>	<i>Pseudocheilinus</i>
Species	<i>varius</i>	<i>bivittatus</i>	<i>rubripinnis</i>	<i>octotenia</i>
variable	(N=10)	(N=8)	(N=6)	(N=7)
TL (mm)	133.50±21.69	144.56±22.98	77.00±3.69	88.00±7.17
\mathcal{AR}	3.49±0.3	2.34±0.46	2.94±0.25	1.52±0.18
S1	1.32±0.06	1.08±0.11	1.21±0.05	0.87±0.05
S6	0.50±0.05	0.65±0.05	0.57±0.07	0.60±0.05
C1	0.78±0.10	0.60±0.06	0.85±0.05	0.47±0.05
C5	0.55±0.12	1.23±0.43	0.41±0.08	2.21±0.19
M1	0.47±0.03	0.59±0.07	0.46±0.02	0.71±0.03
M2	0.52±0.05	0.63±0.05	0.51±0.01	0.73±0.03
M3	0.57±0.04	0.67±0.05	0.56±0.01	0.75±0.01

Values are means ± s.d.

TL, total fish length; \mathcal{AR} , aspect ratio; S1, leading-edge span relative to the square root of fin area; S6, the trailing-edge span relative to the square root of fin area; C1, the mean chord of the first (proximal-most) element relative to the mean chord of the fin; C5, the mean chord of the fifth (distal-most) element relative to the mean chord of the fin; M1, M2, M3, the standardized first, second and third moments of fin area.

The authors apologise for any inconvenience this error may have caused.

Performance limits of labriform propulsion and correlates with fin shape and motion

Jeffrey A. Walker^{1,*} and Mark W. Westneat²

¹*Department of Biology, University of Southern Maine, 96 Falmouth Street, Portland, ME 04103, USA and*

²*Department of Zoology, Field Museum of Natural History, 1400 South Lake Shore Drive, Chicago, IL 60605, USA*

*e-mail: walker@usm.maine.edu

Accepted 8 November 2001

Summary

Labriform locomotion, which is powered by oscillating the paired pectoral fins, varies along a continuum from rowing the fins back and forth to flapping the fins up and down. It has generally been assumed (i) that flapping is more mechanically efficient than rowing, a hypothesis confirmed by a recent simulation experiment, and (ii) that flapping should be associated with wing-shaped fins while rowing should be associated with paddle-shaped fins. To determine whether these hypotheses and the results of the simulation experiment are consistent with natural variation, we compared the steady swimming performance (critical swimming speed) of four species of labrid fish (*Cirrhilabrus rubripinnis*, *Pseudocheilinus octotaenia*, *Gomphosus varius* and *Halichoeres bivittatus*) selected to

form two pairs of closely related species that vary in fin shape and in the direction of fin motion. The results were consistent with expectations. Within each pair, the species with the best swimming performance also had (i) a fin shape characterized by a higher aspect ratio, a longer leading edge relative to the trailing edge fin rays and the center of fin area located closer to the fin base, and (ii) a steeper (more dorsoventral) stroke plane.

Key words: morphometrics, moments of area, locomotion, critical swimming speed, Labridae, fish, swimming, flapping, rowing, *Cirrhilabrus rubripinnis*, *Pseudocheilinus octotaenia*, *Gomphosus varius*, *Halichoeres bivittatus*.

Introduction

There is tremendous diversity in the shape and motion of oscillating wings, fins, legs and feet among animals moving through fluids. Knowing whether and how this variation affects locomotor performance is critical for developing ecological and evolutionary explanations of the variation. For example, recent work has shown that labrid fishes (wrasses and parrotfish) with lower-aspect-ratio paddle-shaped fins tend to swim more slowly (Wainwright et al., 2002) and occupy less energetic zones on the reef (Bellwood and Wainwright, 2001; Fulton et al., 2001) relative to labrids with higher-aspect-ratio wing-shaped fins. In addition, within labrids, paddle-shaped fins tend to row anteroposteriorly along a shallow plane while wing-shaped fins tend to flap dorsoventrally along a steep plane (Bellwood and Wainwright, 2001; Fulton et al., 2001; Wainwright et al., 2002). The association between appendage shape and motion is not unique to fishes but occurs in a diverse array of animal taxa (Fish, 1996; Vogel, 1994; Walker, 2002; Walker and Westneat, 2000). This repeated evolution of rowing, paddle-shaped appendages and flapping, wing-shaped appendages begs an explanation.

It has traditionally been believed on the basis of largely qualitative data that flapping is more mechanically efficient than rowing and, indeed, a computer simulation experiment (Walker and Westneat, 2000) supported this hypothesis. Vogel

(1994) found that rowing generates more thrust at low speeds, a result that has sometimes been interpreted as meaning that rowing is more efficient than flapping at low speeds. Our simulation results did not support this interpretation. Instead, the simulated flapping fin had a higher efficiency than the simulated rowing fin at all speeds. While our simulated rowing fin generated marginally more thrust per stroke cycle than the flapping fin at very low speeds, it generated much more thrust per half-cycle (the power stroke) than the flapping fin over a broad range of speeds. The simulation results suggest, then, that a flapping geometry should be the preferred motion for behaviors requiring conservation of energy while a rowing geometry should be the preferred motion for stopping, starting and yaw turning behaviors, all maneuvers that require a strong power stroke (Walker and Westneat, 2000).

What about fin planform? The optimal shape of a rowing appendage is a distally expanding paddle (Blake, 1981). This design maximizes the region of the fin that contributes to thrust and minimizes the region of the fin that contributes to drag. In contrast, to reduce the relative loss of energy at the distal tip, flapping appendages should taper distally and present relatively high aspect ratios (Combes and Daniel, 2001).

The hypothesis that animals with flapping wings can achieve and sustain higher swimming speeds than animals with rowing

paddles has been explored in numerous studies on the swimming energetics of rowing or flapping turtles, birds and mammals (Fish, 1992, 1993, 1996; Fish et al., 1997; Videler and Nolet, 1990). The results of these studies are reasonably consistent with the hypothesis that flapping is more efficient than rowing, but there are notable exceptions (Fish et al., 1997). One problem with the comparison of animals from broad taxonomic groups is that fundamental differences in behavior and physiology among distantly related taxa can confound the results. A comparison of closely related taxa can potentially minimize the influence of confounding variables. However, morphological and performance differences among closely related taxa will probably not reach the magnitudes measured between extreme forms.

We explored the hypothesis that animals with flapping wings can achieve and sustain higher swimming speeds than animals with rowing paddles by comparing steady swimming ability within two pairs of closely related species of Labridae. At the same time, these data provide critical performance data to support the ecomorphological associations described above (Bellwood and Wainwright, 2001; Fulton et al., 2001; Wainwright et al., 2002). Labrids are a particularly good choice for a comparison of fin shape, fin motion and swimming performance because the family presents extreme diversity in these (and other) phenotypic traits. Initial qualitative observations suggested that, within each of the pairs of species that we studied, at the speeds generally observed in a small aquarium, one member was more at the rowing end of the continuum while the other was more at the flapping end.

Although a fully resolved phylogeny is not yet available, the species within each pair are more closely related to each other than to either member of the other pair. *Cirrhilabrus rubripinnis*, a flapper, and *Pseudocheilinus octotaenia*, a rower, are both members of the pseudocheiline group of the tribe Cheilini (Westneat, 1993). *Gomphosus varius*, a flapper, and *Halichoeres bivittatus*, a rower, are both members of the derived labrid tribe Julidini (Westneat, 1993). By studying close relatives with different behaviors and morphologies, we simultaneously avoided potential problems resulting from the comparison of taxonomically diverse animals and the statistical problems (Felsenstein, 1985) of treating a set of closely related species as independent samples.

We used the hypothesized relationship between fin shape and stroke geometry to guide our initial selection of which species to compare. The goals of the study were (i) to quantify fin shape differences among the species, (ii) to quantify the degree to which a species rows or flaps its fins, (iii) to measure swimming endurance in each species and, finally, (iv) to test the hypothesis that fin shape, the geometry of fin motion and swimming ability are causally related by comparing the distribution of these variables between species within each taxonomic pair. Specifically, we expected that fishes with high pectoral-fin-powered endurance should oscillate high-aspect-ratio distally tapering fins along a steep stroke plane.

Materials and methods

Fin morphometrics

The fins of 10 *Gomphosus varius* Lacepède 1801 (10.5–16.9 cm TL), nine *Halichoeres bivittatus* Bioch 1791 (11.8–18.1 cm TL), six *Cirrhilabrus rubripinnis* Randall and Carpenter 1980 (7.3–8.0 cm TL) and eight *Pseudocheilinus octotaenia* Jenkins 1900 (7.7–10.1 cm TL), where TL is total length, were removed after the individual had been killed with a lethal dose of methane sulfonate salt (IACUC protocol FMNH 97-6). The fins were pinned to a foam board with the rays in an expanded (splayed) position and brushed with full-strength formalin to preserve them in this position. Digital images of the fins were then captured using a Wild M3Z stereomicroscope equipped with a Kodak DC120 digital camera. Digital images were then saved in Photoshop 4.0 and duplicated as TIFF format files for analysis using NIH Image 1.62 on an Apple Macintosh G3 computer.

Both measured and constructed variables that reflect functional aspects of fin shape were measured from each pinned fin. Fin semispan, R , was measured as the length of the leading-edge fin ray (Fig. 1A; the chord between landmarks 1 and 2). Assuming bilateral symmetry, fin aspect ratio, \mathcal{AR} , was computed as $\mathcal{AR}=2R^2/A$, where A is the area of the pinned fin. A measure that reflects whether a fin is distally expanding or tapering is the distribution of spans from leading edge to trailing edge. The fin base and distal edge were divided into five equal parts, lines through corresponding points were constructed and the segments, or spans, between the ray base and ray tips were measured (Fig. 1B). These spans were standardized by the square root of A .

Five curved chords were constructed at equal intervals along the span. The most proximal curved chord is the base of the fin rays (Fig. 1C). Importantly, every point along one of the distal curved chords is an equal distance, r_j , from the basal chord (Fig. 1C). Because the forces and torques of an oscillating fin are a function of the distance from the fin base, we measured these curved chords instead of the more traditional straight chords. A pair of curved chords bounds a fin element, e_j , with area, a_j , that is approximately $\Delta r(c_j+c_{j+1})/2$, where Δr is $R/5$ and c_j is the length of the j th constructed chord (Fig. 1C). Note that $(c_j+c_{j+1})/2$ is the mean chord for element j . Because the fifth (most distal) element is not bounded by a distal chord, we used the measured area of this element for a_5 . The mean chord for the fifth element is $a_5/\Delta r$. Following Ellington (1984), we standardized areas by $\hat{a}_j=(a_j/A)$. The standardized k th moment of area is:

$$\sum_{j=1}^5 \hat{r}_j^k \hat{a}_j,$$

where

$$\hat{r}_j = \frac{r_j - \Delta r}{R}.$$

The first moment of area, M1, is the relative distance of the center of fin area from the fin base and generally indicates whether the fin is 'paddle-shaped' (i.e. distally expanding) or

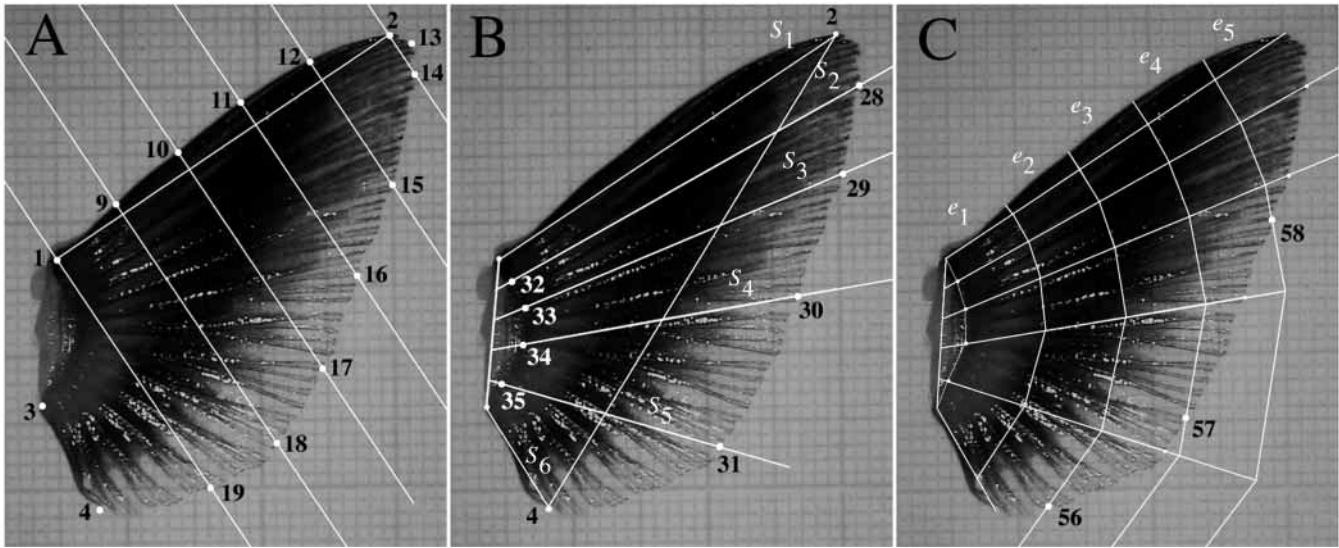


Fig. 1. Morphometrics of fin shape. (A) Landmarks used to compute fin area. (B) Spans, $S_1=S_6$, measured as the length from the base of the fin ray to the tip of the fin rays. (C) Curved chords. The area of the elements, e_j , bounded by the chords was used to estimate the moments of area.

‘wing-shaped’ (i.e. distally tapering). The second moment of area, M_2 , is proportional to aerodynamic (Weis-Fogh, 1973) and inertial (including the acceleration reaction) forces. The third moment of area, M_3 , is proportional to mean profile power (Weis-Fogh, 1973).

Analysis of variance (ANOVA) was used to test for differences in \mathcal{A} and M_1 between *G. varius* and *H. bivittatus* and between *C. rubripinnis* and *P. octotaenia* (the high dependence among moments obviates the need to test for differences in M_2 and M_3). For the comparison of spans, we included all four species in a multivariate ANOVA (MANOVA) model. All statistical tests were performed using JMP 3.1 on an Apple Macintosh G4 computer.

Performance trials and kinematic variables

Individual fish were purchased through tropical marine fish wholesalers in Chicago, USA. Extreme care was taken not to purchase fish that were lethargic or had symptoms of parasite infection. Fish were maintained in 200l aquaria at 25 °C attached to a marine water system containing 2400l of recirculating water. All fish were allowed to acclimate to laboratory tanks for at least 1 week before performance testing.

We used an open-top, circular flow tank (Vogel and LaBarbera, 1978) for all swimming trials. Water temperature in the flow tank was maintained at 25 ± 1 °C. The main compartment of the flow tank has dimensions of 30 cm \times 30 cm \times 120 cm, but the water level in the main compartment was maintained at 25 cm. Initial trials indicated that some fish could effectively avoid high flows by wedging themselves into the square corners of the main compartment. We placed a Plexiglas half-pipe into the main section that proved effective at forcing the fish to swim in the water column. To avoid negative physiological responses to the test tank, prior to each trial, we piped water from one of the reservoirs of the main system into the flow tank. Following

each trial, all water from the flow tank was pumped back into the system.

We used an increasing velocity test to measure critical swimming speed, U_{crit} , which is the maximum speed that can be maintained for a set length of time and is often used as a proxy for the maximum sustained swimming speed (Hammer, 1995). All fish were tested individually to avoid interactions that could reduce performance. A trial was ended when the fish impinged on the downstream grid and could not be stimulated to regain position in the water and swim. For most trials, the flow speed at which the individual could not maintain position using only pectoral fin propulsion was noted. We refer to this speed as U_{p-c} (Drucker and Jensen, 1996a). Prior to placement in the flow tank, estimated body length (EL), measured from the tip of the snout to the posterior margin of the caudal fin, was estimated to the nearest 0.5 cm. Fish were allowed to recover from handling and acclimate to the flow tank for 1 h. Following the rest period, we slowly increased water speed to the initial velocity. In general, the initial velocity was 2 EL s^{-1} . We increased the flow speed at constant increments, relative to body length, at 15 min intervals. For all *G. varius* and *H. bivittatus*, increments were 0.25 EL s^{-1} . Because of their smaller body size, most of the increments for *C. rubripinnis* and *P. octotaenia* were 0.33 EL s^{-1} , although we did use increments of 0.25 EL s^{-1} for some trials. We used 15 min intervals, which is marginally above the minimal time necessary to avoid an artificially inflated U_{crit} (Hammer, 1995). Following the trial, the total length (TL) was measured.

Finally, we measured the maximum speed, U_{p-max} , that an individual could achieve in the flow using only labriform propulsion. To measure U_{p-max} , we used an increasing velocity test in which the speed of the flow was increased by increments of approximately 2.2 cm s^{-1} once it had been determined whether the individual could maintain position over several fin-beat cycles by using only the pectoral fins to generate thrust.

$U_{p\text{-max}}$ was taken as the final speed prior to the speed at which the individual failed to maintain position. $U_{p\text{-max}}$ differs from $U_{p\text{-c}}$ in that the former is a measure of the sprint capacity of the pectoral fins while the latter is a measure of the prolonged swimming capacity of the pectoral fins.

Following at least 1 day of recovery from the increasing velocity test, fish were filmed swimming at a range of speeds in the flow tank following the protocol in Walker and Westneat (1997). Fin beats were digitized using a modification of the public domain NIH Image program (developed at the US National Institutes of Health and available at <http://rsb.info.nih.gov/nih-image/>). From the digitized sequences, five kinematic variables were constructed: frequency of the stroke cycle, stroke angle, stroke plane angle, abduction angle and adduction angle.

The stroke angle, ϕ , is the maximum angular displacement of the leading-edge ray over the fin beat. ϕ was measured as the angle between the three-dimensional vectors representing the position of the distal tip of the leading-edge ray, with its base at the origin, at maximum adduction and maximum abduction. Because the data were digitized from a two-dimensional lateral view, the coordinates of the third dimension had to be reconstructed. The x (dorsoventral) and z (mediolateral) anatomical axes were aligned with the horizontal and vertical axes of the computer monitor, respectively. At maximum adduction (positioned back against the body), it was assumed that the fin ray was in the xz plane (i.e. $y=0$), and the length of the ray was computed. At maximum abduction, the y component was estimated from the measured length of the ray and the digitized x and z components.

The error in this method will increase with the magnitude of the spanwise deformation of the fin ray at maximum abduction. We were able to estimate the error by comparing these two-dimensional estimates with the three-dimensional estimates for

G. varius, since these two-dimensional coordinate data were simply the subset of the full three-dimensional data described by Walker and Westneat (1997). The median absolute error is 3.5° . There is no bias in the direction of the difference; the mean error ($\phi_{3D}-\phi_{2D}$) is -0.7066° , which does not differ from zero (Wilcoxon signed-rank test).

The stroke plane angle, β , is the angle between the path of fin movement in the xz plane and a unit z (or dorsoventral) vector (Jensen, 1956). Following Walker and Westneat (1997), we use the slope, b , of the major axis of the path of the tip of the leading-edge ray to describe the slope of fin movement. β is then found from $\beta=(\pi/2)-\tan^{-1}b$. Prior to computing β , the digitized points were smoothed with a quintic spline (Walker, 1998a) and interpolated to 100 points using the software QuicCurve (Walker, 1998b).

The abduction and adduction strokes were not swept out on the same plane; the abduction stroke plane was always steeper than the adduction stroke plane. That is, the fin tended to sweep down during abduction, whereas the fin tended to sweep back during adduction. We therefore computed separate stroke plane angles for the abduction and adduction strokes. We refer to these as the down (β_{down}) and up (β_{up}) stroke plane angles. The down and up stroke planes were estimated from the line segment in the xz plane spanning the points that were 25% and 75% of the distance along the abduction or adduction curve. Down and up stroke angles were computed as the angle between these line segments and the unit z vector.

Statistical tests for performance and kinematic data

For most analyses, kinematic variables varied with swimming speed, which would suggest that species effects should be tested with analysis of covariance (ANCOVA) with speed as the covariate. Because of a significant speed \times species interaction (i.e. the slope of kinematics against speed differed among species), however, we could not use a standard

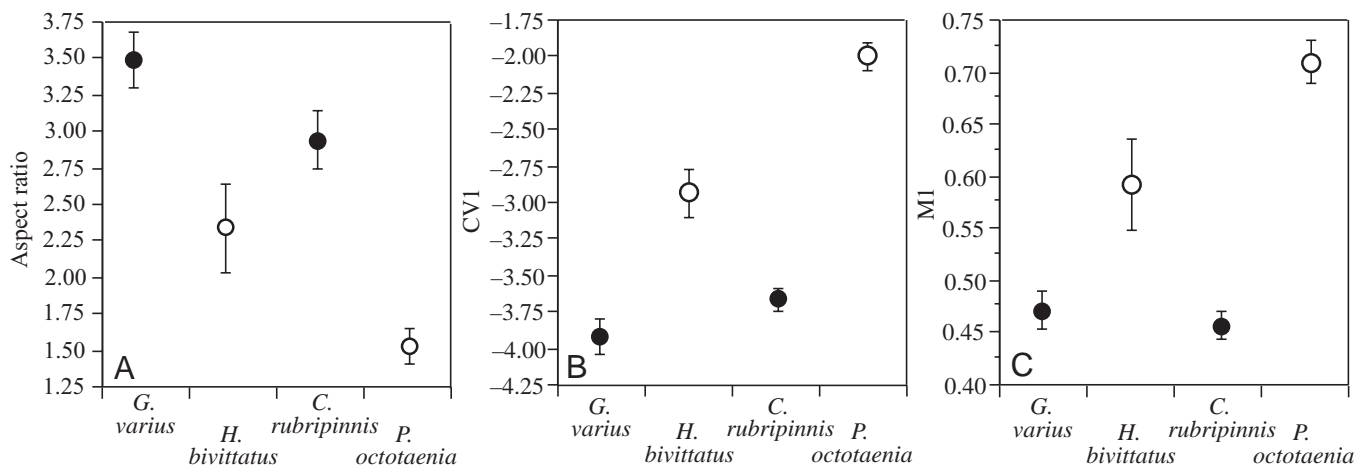


Fig. 2. Distribution of composite functional shape variables. (A) Aspect ratio of the pectoral fin. (B) First canonical variate of size-standardized span data. (C) First standardized moment of area (relative distance of center of fin area from fin base) of the pectoral fins. Value in are means ± 2 S.E.M. The species represented by filled circles are 'flappers' while the species represented by open circles are 'rowers.' Sample sizes, N , are given in Table 1.

Table 1. Fin shape data for four species of labrid fish

Species variable	<i>Gomphosus varius</i> (N=10)	<i>Halichoeres bivittatus</i> (N=8)	<i>Cirrhitilabrus rubripinnis</i> (N=6)	<i>Pseudocheilinus octotaenia</i> (N=7)
TL (mm)	133.50±21.69	144.56±22.98	77.00±3.69	88.00±7.17
\mathcal{R}	3.49±0.3	2.34±0.46	2.94±0.25	1.52±0.18
S1	1.32±0.06	1.08±0.11	1.21±0.05	0.87±0.05
S6	0.50±0.05	0.65±0.05	0.57±0.07	0.60±0.05
C1	0.78±0.10	0.60±0.06	0.85±0.05	0.47±0.05
C5	0.55±0.12	1.23±0.43	0.41±0.08	2.21±0.19
M1	0.47±0.03	0.59±0.07	0.46±0.02	0.71±0.03
M2	0.52±0.05	0.63±0.05	0.51±0.01	0.73±0.03
M3	0.57±0.04	0.67±0.05	0.56±0.01	0.75±0.01

Values are means \pm S.D.

TL, total fish length; \mathcal{R} , aspect ratio; S1, leading-edge span relative to the square root of fin area; S6, the trailing-edge span relative to the square root of fin area; C1, the mean chord of the first (proximal-most) element relative to the mean chord of the fin; C5, the mean chord of the fifth (distal-most) element relative to the mean chord of the fin; M1, M2, M3, the standardized first, second and third moments of fin area.

ANCOVA model to test for kinematic differences within each rower/flapper pair. Instead, we used a non-parametric test similar in spirit to ANCOVA. This test was designed to answer the question, 'while swimming at a speed of $X TL s^{-1}$, does the kinematic variable Y differ between species A and species B?' Specifically, we compared the kinematics at the minimum and maximum speeds in which kinematic variables were measured for both species in each comparison.

For a specific comparison, we used a quadratic regression, fitted separately within each species, to compute the expected value of the kinematic variable at either the lowest

or highest swimming speed. The difference between expected values was our test statistic, and a permutation test was used to test its significance. Given a data matrix with species in the first column, swimming speed in the second column and a kinematic variable in the third column, we randomly permuted the cells of the first column and then recomputed the regressions for each pseudogroup and the associated pseudodifference at either the minimum or maximum speed. We performed this permutation and recalculation of the pseudodifference 9999 times and compared the test statistic with the distribution of the 10 000 pseudodifferences (one of which was the observed difference). If the test statistic lay outside the 95% confidence intervals of the distribution, we considered the test statistic significant.

Because of the large body length variation in the *G. varius* and *H. bivittatus* tested and because swimming performance varied with body length, it was necessary to use an ANCOVA model, with body length as the covariate, to test for differences in their swimming performance. A significant species \times body length interaction precluded the use of a standard ANCOVA model. Instead, we used the permutation algorithm described above. For these data, the permutation test addressed the question, 'at length X , does swimming performance differ between species A and species B?'. We compared performance at the size of the smallest and largest measured fish in the pair of species.

For the comparison of performance between *P. octotaenia* and *C. rubripinnis*, we used a permutation test similar to that described above but, in this case, the difference in the mean performance between species and pseudogroups was the test statistic since these species varied little in body length. The permutation test for this comparison, then, was similar in spirit to a t -test.

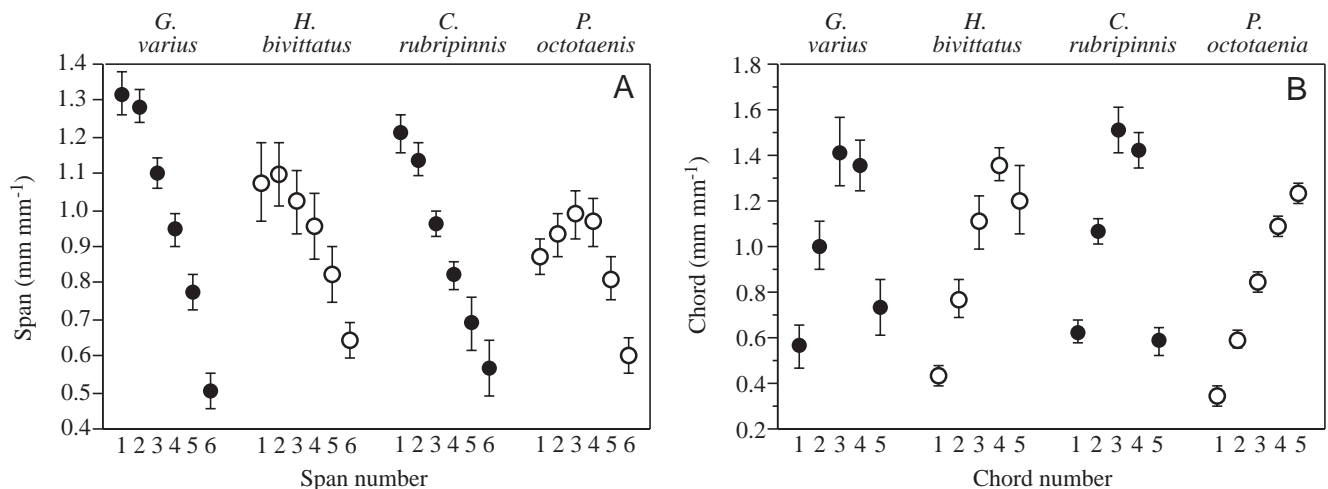


Fig. 3. Span and chord distributions of the pectoral fin. (A) Mean of spans are standardized by the square root of fin area. The spans are ordered (1–6) from leading to trailing edge. (B) Means of curved chords standardized by mean curved chord. The chords are ordered (1–5) from proximal to distal. Value are means ± 1 S.E.M. The species represented by filled circles are 'flappers' and the species represented by open circles are 'rowers'. Sample sizes, N , are given in Table 1.

Results

We found significant differences in fin planform, fin kinematics and swimming performance between the two species in each comparison. The major trend in our data is that labriform swimmers with more elongate, wing-like fins and with a steeper (more dorso-ventral) stroke plane can achieve and maintain higher swimming speeds than can labriform swimmers with lower-aspect-ratio paddle-like fins and shallower stroke planes.

Fin shape analysis

The aspect ratio in the four species ranged from approximately 1.5 in *P. octotaenia* to 3.5 in *G. varius* (Table 1) (Fig. 2A). As expected, \mathcal{AR} in *G. varius* was significantly greater than in *H. bivittatus* ($F=42.5$, $P<0.0001$) and that in *C. rubripinnis* was significantly greater than in *P. octotaenia* ($F=156.6$, $P<0.0001$).

The distribution of relative fin spans (span over the square root of area) from leading edge to trailing edge was also different among species (Fig. 3A). The fin spans of *G. varius* and *C. rubripinnis* are more asymmetric, as indicated by the relative lengths of the leading- and trailing-edge spans, than those of *H. bivittatus* and *P. octotaenia*. In addition, the leading-edge span (completed by the second fin ray) is longest in *G. varius* and *C. rubripinnis* while the second or third span is longest in *H. bivittatus* and *P. octotaenia* (Fig. 3A). The pattern of loadings on the first canonical variate of the spans data indicates that the major axis of shape difference among the four species reflects a contrast between the relative lengths of the anterior and posterior spans (the canonical loadings, or correlations between the first canonical variate and the original variables are, from leading to trailing edge, -0.99 , -0.95 , -0.43 , 0.52 , 0.63 and 0.66 , respectively). Scores on the first canonical variate (Fig. 2B) show that both *G. varius* and *C. rubripinnis* have long anterior spans relative to posterior spans, *P. octotaenia* has relatively short anterior spans and *H. bivittatus* has relatively intermediate anterior spans. Scores on the first canonical variate differ significantly between *G. varius* and *H. bivittatus* ($F=85.5$, $P<0.0001$) and between *C. rubripinnis* and *P. octotaenia* ($F=649.7$, $P<0.0001$).

The fins of *G. varius* and *C. rubripinnis* taper substantially (that is, chord lengths decrease) distal to the third chord, while the fin of *H. bivittatus* tapers only distal to the fourth chord and the fin of *P. octotaenia* fails to taper at all (Fig. 3B). This variation in shape is reflected in the first to third moments of area (Table 1). The first moment (or center) of area is nearer the fin base in *G. varius* and *C. rubripinnis*, nearer the distal edge in *P. octotaenia* and has a more intermediate location in *H. bivittatus* (Table 1) (Fig. 2C). The first moment differs significantly between *G. varius* and *H. bivittatus* ($F=27.6$, $P<0.0001$) and between *C. rubripinnis* and *P. octotaenia* ($F=379.8$, $P<0.0001$) (Fig. 2C).

Kinematics

The stroke plane angle, β , decreased significantly (became steeper or more dorso-ventral) with speed in *H. bivittatus* ($P\leq 0.0001$) and *P. octotaenia* ($P\leq 0.0001$) but not in *G. varius*

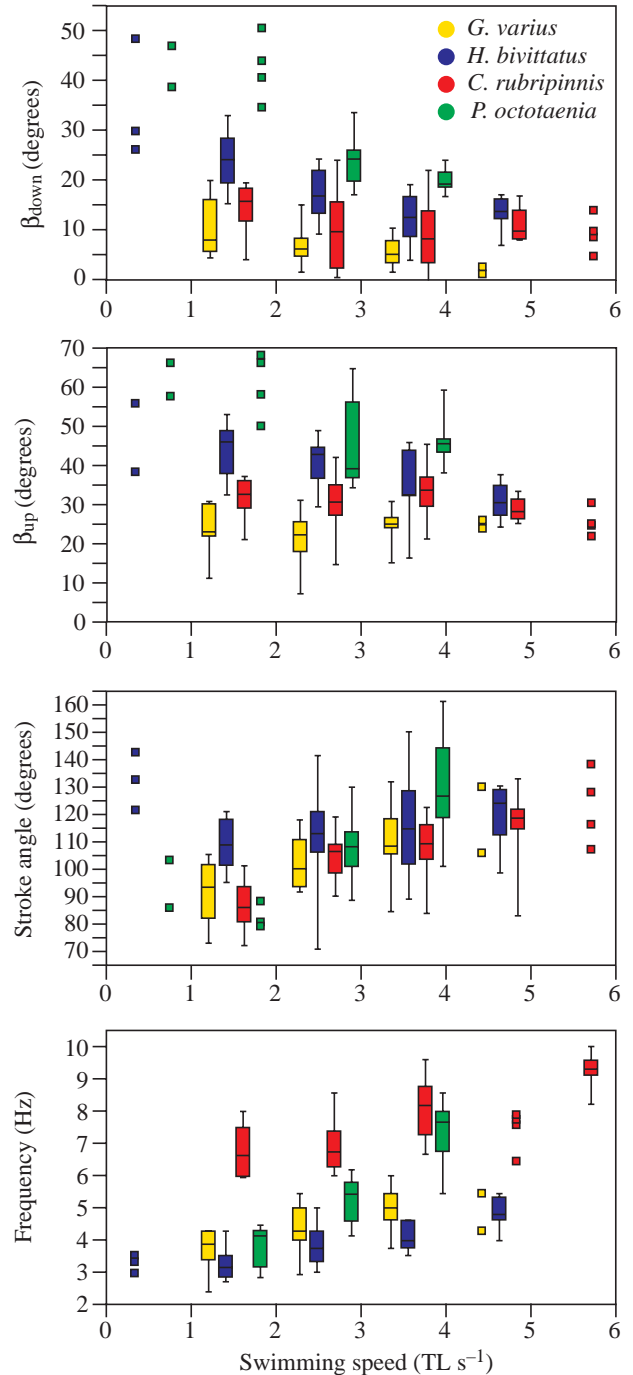


Fig. 4. (A–D) Kinematic changes with swimming speed in four labrid species. Each box-and-whisker plot represents the distribution of the variable for the species. The median of the distribution is represented by the line within the box. The 25th and 75th percentiles are represented by the top and bottom box edges, respectively. The 10th and 90th percentile are represented by the top and bottom caps on the vertical lines (whiskers) outside the box, respectively. If the sample is too small for a box plot, each measurement is simply represented by a square box. The numbers of individuals, N_i , and sequences, N_s , were as follows: *Gomphosus varius*, $N_i=3$, $N_s=29$; *Halichoeres bivittatus*, $N_i=5$, $N_s=69$; *Cirrhilabrus rubripinnis*, $N_i=6$, $N_s=69$; *Pseudocheilinus octotaenia*, $N_i=4$, $N_s=34$. TL, total fish length.

Table 2. Kinematic comparisons at the low and high ends of the swimming speed range

	Speed (TL s ⁻¹)	<i>Halichoeres bivittatus</i>	<i>Gomphosus varius</i>	<i>P</i>
β (degrees)	1.4	36.2	16.7	≤ 0.0001
	4.3	22.4	16.7	0.034
β_{down} (degrees)	1.4	26.2	10.2	≤ 0.0001
	4.3	12.5	2.7	0.0108
β_{up} (degrees)	1.4	44.6	23.3	0.0001
	4.3	31.4	23.3	0.172
ϕ (degrees)	1.4	110.4	91.1	0.0003
	4.3	119.2	120.1	0.2748
<i>f</i> (Hz)	1.4	3.7	3.3	0.5067
	4.3	5.4	4.6	0.3847

	Speed (TL s ⁻¹)	<i>Pseudochilinus octotaenia</i>	<i>Cirrhilabrus rubripinnis</i>	<i>P</i>
β (degrees)	1	47.2	22.4	0.0002
	3.9	30.1	22.4	0.0008
β_{down} (degrees)	1	36.8	12.6	0.0006
	3.9	14.2	9.4	0.0109
β_{up} (degrees)	1	56.5	33.1	0.0002
	3.9	41.4	29.3	0.007
ϕ (degrees)	1	91.9	89.8	0.2764
	3.9	134.3	113.8	0.0019
<i>f</i> (Hz)	1	3.1	6.4	0.0024
	3.9	7.9	8.9	0.065

Stroke plane angles for entire stroke (β) and for each half-stroke independently (β_{down} and β_{up}) are shown.

The angles are between the projection of the stroke plane onto the sagittal (xz) plane and the dorsoventral (z) axis.

ϕ is the stroke angle (twice the stroke amplitude); f is the stroke frequency; TL, total fish length.

P values are from a permutation ANCOVA test (described in Materials and methods).

($P=0.24$) or *C. rubripinnis* ($P=0.0645$). Downstroke plane angles decreased significantly with speed in all four species (*H. bivittatus*, $P\leq 0.0001$; *G. varius*, $P\leq 0.0044$; *P. octotaenia*, $P\leq 0.0001$; *C. rubripinnis*, $P\leq 0.0393$), although the magnitude of the decrease was much smaller in *G. varius* and *C. rubripinnis* (Fig. 4) (Table 2). The upstroke plane angle decreased significantly with speed in all species but *G. varius* (*H. bivittatus*, $P\leq 0.0001$; *G. varius*, $P=0.344$; *P. octotaenia*, $P=0.0009$; *C. rubripinnis*, $P=0.028$), but the magnitude of the change was much smaller in *C. rubripinnis* than in either *H. bivittatus* or *P. octotaenia* (Fig. 4) (Table 2).

We were able to measure stroke plane angles at lower speeds in *H. bivittatus* and *P. octotaenia* than in *G. varius* or *C. rubripinnis*. At the lowest speed measured for *G. varius* (1.42 TL s^{-1}), *H. bivittatus* had significantly shallower stroke plane and downstroke and upstroke angles than *G. varius* (Fig. 4) (Table 2). Similarly, *P. octotaenia* had significantly shallower stroke plane and downstroke and upstroke angles than *C. rubripinnis* at the lowest swimming speeds (Fig. 4) (Table 2).

The maximum speed at which kinematic data were measured for both *H. bivittatus* and *G. varius* was 4.3 TL s^{-1} , which is above the expected U_{crit} for even the smallest *H. bivittatus* individuals (Fig. 4) (Table 2). At this relative speed, the stroke plane and downstroke angles were significantly shallower in *H. bivittatus*, but the upstroke angle was not (Fig. 4) (Table 2). The maximum speed at which kinematic data were measured for *P. octotaenia* was 3.9 TL s^{-1} , only 0.1 TL s^{-1} less than the mean U_{crit} for this species (Table 2) (Fig. 5). At this speed, the stroke plane and downstroke and upstroke angles were significantly shallower in *P. octotaenia* than in *C. rubripinnis* (Fig. 4) (Table 2).

The stroke angle increased with speed in all four species (*H. bivittatus*, $P=0.049$; *G. varius*, $P=0.003$; *P. octotaenia*, $P\leq 0.0001$; *C. rubripinnis*, $P\leq 0.0001$). *H. bivittatus* had a larger stroke angle than *G. varius* at low swimming speeds, but no differences occurred at high swimming speeds (Fig. 4) (Table 2). In contrast, the stroke angles of *P. octotaenia* and *C. rubripinnis* did not differ at low swimming speeds, but the

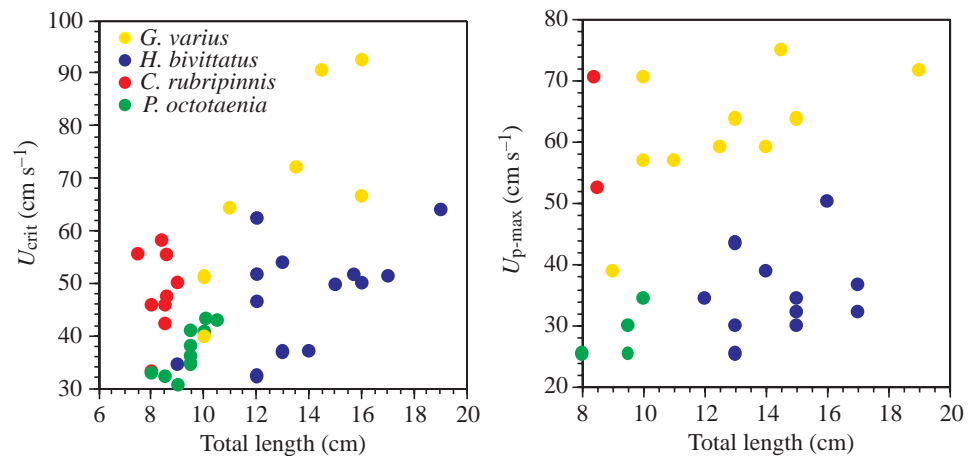


Fig. 5. (A) Critical swimming speed, U_{crit} , and (B) maximum pectoral-fin-powered speed, $U_{\text{p-max}}$, for the individuals of the four labrid species.

stroke angle of *P. octotaenia* was greater than that of *C. rubripinnis* at high speeds.

Oscillation frequency increased in all four species (*H. bivittatus*, $P \leq 0.0001$; *G. varius*, $P \leq 0.0001$; *P. octotaenia*, $P \leq 0.0001$; *C. rubripinnis*, $P \leq 0.0001$). Frequency did not differ between *H. bivittatus* and *G. varius* at either low or high speed (Fig. 4) (Table 2). *C. rubripinnis* had much greater frequencies than *P. octotaenia* at low speeds (1 TL s^{-1}), but this difference vanished near the critical swimming speed of *P. octotaenia* (3.9 TL s^{-1}).

Swimming performance

The four labrid species studied here employed their pectoral fins for steady forward locomotion throughout the critical swimming speed trials. At the fatigue velocities, all four species used their body and tail in a rapid undulation to regain an upstream position, and then attempted to maintain position with only the pectoral fins. These axial 'kicks' were characterized by 1–4 cycles of large-amplitude undulation with the median fins and caudal fin fully erect. No individual was observed maintaining position with this axial mode; instead, axial kicking always resulted in rapid forward translation relative to the fixed tank. In addition, all fish used a burst of axial undulation at slow speeds in a behavior that is characteristic of a fish seeking out a refuge. At higher swimming speeds, fishes maintained velocity without this exploratory behavior. *C. rubripinnis* and *P. octotaenia* undulated their dorsal fins at slow speeds, but at higher speeds the dorsal fin, together with the anal fin, was retracted against the body. Because oscillation frequencies at high swimming speeds do not differ between species within each comparison (see above), relative stride lengths (relative swimming speed divided by oscillation frequency) at high speeds also do not differ between species within each comparison.

Critical swimming speeds (Table 3) (Fig. 5) increased with body length in both *H. bivittatus* ($U_{\text{crit}} = 20.7 + 1.95 \text{ TL}$, $P = 0.03$) and *G. varius* ($U_{\text{crit}} = 0.346 + 5.23 \text{ TL}$, $P = 0.003$). $U_{\text{p-max}}$ increased with body length in *G. varius* ($U_{\text{p-max}} = 34.9 + 2.1 \text{ TL}$, $P = 0.03$) but not in *H. bivittatus* ($P = 0.24$). *G. varius* had a

Table 3. Expected critical swimming speed (U_{crit}) and maximum pectoral-fin-powered swimming speed ($U_{\text{p-max}}$) at the high and low end of the size range for *Gomphosus varius* and *Halichoeres bivittatus*

	TL			
	(mm)	<i>H. bivittatus</i>	<i>G. varius</i>	<i>P</i>
U_{crit} (cm s^{-1})	9	38.2	47.4	0.1447
	16	52.0	84.0	0.0033
$U_{\text{p-max}}$ (cm s^{-1})	12	35.5	60.1	≤ 0.0001
	17	37.5	70.6	≤ 0.0001

TL, total fish length.

The expected value at a specific size is based on the coefficients from a least-squares regression of U_{crit} on TL.

The *P* value is from a permutation ANCOVA test for the difference in expected value.

Table 4. The mean U_{crit} and $U_{\text{p-max}}$ for the *Cirrhilabrus rubripinnis* and *Pseudocheilinus octotaenia* comparison

	Mean TL (mm)	U_{crit} (cm s^{-1})	<i>P</i>
<i>C. rubripinnis</i>	8.1	49.0	≤ 0.0001
<i>P. octotaenia</i>	9.2	37.3	

	Mean TL (mm)	$U_{\text{p-max}}$ (cm s^{-1})	<i>P</i>
<i>C. rubripinnis</i>	8.2	61.7	0.0357
<i>P. octotaenia</i>	9.2	27.9	

The *P* value is from a permutation *t*-test.

TL, total fish length; U_{crit} , critical swimming speed; $U_{\text{p-max}}$, pectoral-fin-powered swimming speed.

higher critical swimming speed than *H. bivittatus* at the longest but not at the shortest body length (Table 3) (Fig. 5). *G. varius* was able to reach a higher $U_{\text{p-max}}$ than *H. bivittatus* at all body lengths (Table 3) (Fig. 5). *C. rubripinnis* had a significantly higher U_{crit} ($P \leq 0.0001$) and $U_{\text{p-max}}$ ($P \leq 0.0357$) than *P. octotaenia* (Table 4) (Fig. 5).

We also noted the speed at which some of the individuals began to rely on intermittent axial kicking to regain position. Drucker and Jensen (1996b) referred to this speed as $U_{\text{p-c}}$. Intermittent axial kicking augmented the critical swimming speeds of some species above those that be maintained with the pectoral fins working alone. The mean percentage difference between U_{crit} and $U_{\text{p-c}}$ was 9.1% in *H. bivittatus*, 0% in *G. varius*, 12.4% in *P. octotaenia* and 3.7% in *C. rubripinnis*. While adjusting U_{crit} to reflect only pectoral-fin-powered swimming speeds (i.e. $U_{\text{p-c}}$) would increase the speed differences between the flappers, *G. varius* and *C. rubripinnis*, and the rowers, *H. bivittatus* and *P. octotaenia*, we did not make this comparison as the test would have less power than the comparison of U_{crit} values because of smaller sample sizes.

Discussion

A major goal of our research is to understand the functional basis of performance variation among fishes swimming in the labriform mode. Drucker and Lauder (2000) addressed this issue by describing differences in the wake geometry between a relatively fast (the black surfperch *Embiotoca jacksoni*) and a relatively slow (the bluegill sunfish *Lepomis macrochirus*) species. They showed that, among other differences, the momentum jet within the reversed von Karmen vortex street (Anderson et al., 1998; Freymuth, 1988) was directed more caudally in *E. jacksoni* but more laterally in *L. macrochirus*. The results presented here are complementary to those of Drucker and Lauder (2000); wake differences must reflect fin shape and motion differences and *vice versa*. Our results identify morphological design correlates of cruising performance. Both high-speed high-endurance species had distally tapered, high-aspect-ratio pectoral fins that

articulated with the body at low angles relative to the two species with lower speed and lower endurance. In addition, we found that fishes designed to have a more flapping stroke can achieve and maintain higher swimming speeds than fishes designed to have more of a rowing stroke. However, the difference between stroke geometry at fatigue velocities varies only slightly between fishes with the two different designs.

Mechanical design and fin shape

Our data show that fin shape varies with kinematics and swimming performance in the direction predicted in the Introduction. Aspect ratio is highest and first moments of area are lowest in *G. varius* and *C. rubripinnis*, the two species with the most vertical stroke plane and the two that can achieve and maintain the highest pectoral-fin-powered swimming speeds. The size-specific first moment of area and the first canonical variate of the size-specific span data are measures of static fin shape; specifically, the degree to which a fin is wing-shaped (tapers distally) or paddle-shaped (expands distally). As stressed by Lauder and Jayne (1996), fin geometry changes substantially throughout the fin stroke as a consequence of both internal and external loads, and the shape of the active fin is most relevant to its function. Nevertheless, the shape of an actively oscillating fin is limited by the features of the fin that we measured: the aspect ratio, the distribution of fin chords and the distribution of fin spans. Thus, it is not surprising that we measured significant correlations between static fin shape and swimming performance.

The Labridae is one of the largest families of reef fish, with over 500 named species, and exhibits high levels of diversity in body shape, pectoral fin shape and locomotor behavior. Using the same morphometric protocol presented here, current studies of the diversity of pectoral fin shape in the Labridae show extremes in fin morphology across species as well as strong intraspecific trends in fin shape with body size (Wainwright et al., 2002). Integration of key locomotor characters such as fin shape with a phylogeny of the family may provide evidence for multiple independent origins of locomotor strategies in different labrid clades (Westneat, 1997).

Stroke shape and performance differences

Many different structural and physiological factors can account for performance differences among species. Instead of measuring detailed kinematics in each of these species and exploring for associations between kinematic features and performance, we used our previous work on simulated fins to make a precise prediction between one aspect of fin kinematics and performance. Specifically, we expected swimming performance to vary with stroke plane angle. To reject the possibility that performance differences were simply a function of either stroke angle or frequency, however, we also measured these variables in all four species. Swimming speed should increase with both the frequency and amplitude of the fin stroke. At the fatigue velocities of the rowers, however, no difference occurred between the stroke angle of *H. bivittatus* and *G. varius*, the stroke angle of *P. octotaenia* was greater

than that of *C. rubripinnis*, frequencies were greater in *H. bivittatus* than in *G. varius*, and no differences in frequency were observed between *P. octotaenia* and *C. rubripinnis*. These results suggest that stroke angle and fin-beat frequency cannot account for the superior swimming performance of *G. varius* and *C. rubripinnis*.

Within each species pair, the species with the steeper stroke plane at maximum speed had significantly higher U_{crit} and U_{p-max} values than the species with the shallower stroke plane, which supports the hypothesis that fishes that flap their fins should be able to achieve and maintain higher pectoral-fin-powered swimming speeds than fishes that row. Interestingly, however, while the dynamic shape of the fin stroke, measured as downstroke and upstroke plane angles, differed greatly between rowers and flappers at slow speeds, the angles of fin motion differed by only 5–12° at speeds near fatigue velocities. That there are small but significant differences in stroke plane angle at higher speeds should not be surprising since we have compared relatively closely related fishes. *H. bivittatus* and *P. octotaenia* should more properly be classified as labriform generalists, given their ability to modify stroke plane angle with swimming speed.

Is the decrease in stroke plane angle with increasing swimming speed in *H. bivittatus* and *P. octotaenia* (Fig. 4) necessary for increased thrust generation or is it a strategy to maintain high mechanical efficiency across a broad range of speeds? Walker and Westneat (2000) showed that a flapping stroke is much more mechanically efficient than a rowing stroke across all swimming speeds, which suggests that the change in stroke plane angle is necessary for increased thrust generation.

There are two fundamental ways that a pair of rowing fins can modify their dynamic shape to generate the increased thrust necessary to balance parasite drag as swimming speed increases: the amplitude and/or frequency can increase enough to maintain a thrust component of the net force during adduction (backstroke) or they can begin to oscillate with a vertical component in order to generate additional thrust during abduction. A fin abducting with a downward component will generate lift in addition to thrust. Confining the vertical motion to abduction produces a net lift over the stroke cycle. Negatively buoyant fish could potentially use this stroke geometry to compensate for the downward force on the body. For neutrally buoyant fish, adducting the fin with the appropriate upward component will produce zero net lift.

Because the horizontal component of the local flow increases with swimming speed, a fin abducting with a shallow stroke plane angle must simultaneously increase its cycle frequency and steepen its stroke plane to maintain thrust generation at increasingly higher swimming speeds. This is essentially how many insects control the stroke plane angle from slow to fast forward flight, although insects generally modify the stroke plane angle by tilting their body (Dudley, 2000). *H. bivittatus* and *P. octotaenia* also appear to employ the strategy of generating larger forces at higher speeds by decreasing the stroke plane angle (making it steeper). In

contrast, a decrease in stroke plane angle with increasing swimming speed is not necessary for fishes with fins that always oscillate with steep stroke planes. Instead, these flapping fins can generate more thrust simply by simultaneously increasing cycle frequency and the magnitude of the pitch of the fin chords. *G. varius* (Walker and Westneat, 1997) and probably *C. rubripinnis* employ this alternative strategy. The high species number and diversity of fin designs in the family Labridae make this an excellent group for examining alternative strategies for achieving high swimming performance.

Why is there variation in fin shape and motion among species?

Given that the flapping gait is more mechanically efficient than the rowing gait at all speeds (Walker and Westneat, 2000), why do *H. bivittatus* and *P. octotaenia* not flap their fins at low speeds? The pectoral fins of *H. bivittatus* and *P. octotaenia* appear to be designed for the wide range of motions between rowing and flapping. For example, the more vertical articulation of the pectoral fin, relative to that of *G. varius* and *C. rubripinnis*, should facilitate a more fore–aft motion. The range of motions observed in *H. bivittatus* and *P. octotaenia* may allow these fish to match fin motion with functional requirement. A stroke along a shallow stroke plane should be able to generate large fore–aft forces without large lift, which might be advantageous for rapid pectoral-fin-powered starts, stops and lateral turns. A shallow stroke plane might also facilitate the ability to hover and swim at slower speeds because of the alternating directions of the net force between power and recovery strokes. While *H. bivittatus* and *P. octotaenia* hover easily, *G. varius* must pitch its body upwards at a large angle to hover for a short duration, a behavior that mimics that of many insects (Dudley, 2000). With increasing swimming speed, the steeper stroke plane should allow the fish to generate large enough forces to balance the increased parasite drag and to swim more efficiently.

Interestingly, the rowing design of the pectoral fin in *H. bivittatus* and *P. octotaenia* is not as extreme as that in the threespine stickleback *Gasterosteus aculeatus*. As in labrids, *Gasterosteus aculeatus* employs an exclusively labriform gait until fatigue velocities are reached (Taylor and McPhail, 1986; Whoriskey and Wootton, 1987). Unlike *H. bivittatus* and *P. octotaenia*, however, *Gasterosteus aculeatus* employs a remarkably stereotypical rowing stroke at all speeds (Walker, 1999). The kinematic and morphological data, then, suggest that *H. bivittatus* and *P. octotaenia* are labriform swimming generalists and may be able to exploit the advantages of both rowing and flapping, but at some cost to cruising performance.

The correlated variation measured here is consistent with the experimental simulation results showing that flapping appendages should be able to achieve and maintain higher speeds than rowing appendages (Walker and Westneat, 2000). A further question worth pursuing is how extremes in appendage shape and motion differ in generating forces and

how these differences are related to net thrust and mechanical efficiency. We agree with Dickinson (1996) that ‘drag-based’ versus ‘lift-based’ is too simple of a model. Wake studies offer a good summary of the interaction between appendage and fluid, and there is some research on how wakes vary among animals with different performance (Drucker and Lauder, 2000). Mechanistic physiologists have developed computational fluid dynamic and robotic models to identify the fluid dynamic mechanisms exploited by flying insects (Birch and Dickinson, 2001; Dickinson et al., 1999; Ellington et al., 1996; Liu et al., 1998; Van den Berg and Ellington, 1997) or to explore optimal motions for generating lift efficiently (Anderson et al., 1998; Archer et al., 1979). These mechanistic studies have addressed how a structure works but not why structural variation exists. The conspicuous presence of rowing paddles and flapping wings among aquatic animals (Fish, 1996; Vogel, 1994; Walker, 2002; Walker and Westneat, 2000) and the growing database demonstrating behavioral and ecological correlates of rowing and flapping (Bellwood and Wainwright, 2001; Fish, 1996; Fulton et al., 2001; Wainwright et al., 2002; Walker and Westneat, 2000) offer evolutionary physiologists the opportunity to exploit these mechanistic physiological techniques to explore the problem of why variation exists.

We would like to thank three anonymous reviewers for greatly improving the focus of the manuscript. We thank D. Dudek for his work on filming fish swimming and M. Alfaro, R. Blob, J. Janovetz, L. Rosenberger and B. Wright for their discussions of this project. This work was funded by a National Science Foundation Postdoctoral Fellowship in the Biosciences Related to the Environment, Office of Naval Research grant N00014-99-0184 to M.W.W. and J.A.W. and National Science Foundation grants IBN-9407253 and DEB-9815614 to M.W.W.

References

- Anderson, J. M., Streitien, K., Barrett, D. S. and Triantafyllou, M. S. (1998). Oscillating foils of high propulsive efficiency. *J. Fluid Mech.* **360**, 41–72.
- Archer, R. D., Sapuppo, J. and Betteridge, D. S. (1979). Propulsion characteristics of flapping wings. *Aeronaut. J.* **83**, 355–371.
- Bellwood, D. R. and Wainwright, P. C. (2001). Locomotion in labrid fishes: implications for habitat use and cross-shelf biogeography on the Great Barrier Reef. *Coral Reefs* **20**, 139–150.
- Birch, J. M. and Dickinson, M. H. (2001). Spanwise flow and the attachment of the leading-edge vortex on insect wings. *Nature* **412**, 729–733.
- Blake, R. W. (1981). Influence of pectoral fin shape on thrust and drag in labriform locomotion. *J. Zool., Lond.* **194**, 53–66.
- Combes, S. A. and Daniel, T. L. (2001). Shape, flapping and flexion: wing and fin design for forward flight. *J. Exp. Biol.* **204**, 2073–2085.
- Dickinson, M. H. (1996). Unsteady mechanisms of force generation in aquatic and aerial locomotion. *Am. Zool.* **36**, 537–554.
- Dickinson, M. H., Lehmann, F.-O. and Sane, S. P. (1999). Wing rotation and the aerodynamic basis of insect flight. *Science* **284**, 1954–1960.
- Drucker, E. G. and Jensen, J. S. (1996a). Pectoral fin locomotion in the striped surfperch. I. Kinematic effects of swimming speed and body size. *J. Exp. Biol.* **199**, 2235–2242.
- Drucker, E. G. and Jensen, J. S. (1996b). Pectoral fin locomotion in the striped surfperch. II. Scaling swimming kinematics and performance at a gait transition. *J. Exp. Biol.* **199**, 2243–2252.
- Drucker, E. G. and Lauder, G. V. (2000). A hydrodynamic analysis of fish

- swimming speed: wake structure and locomotor force in slow and fast labriform swimmers. *J. Exp. Biol.* **203**, 2379–2393.
- Dudley, R.** (2000). *The Biomechanics of Insect Flight*. Princeton: Princeton University Press.
- Ellington, C. P.** (1984). The aerodynamics of hovering insect flight. IV. morphological parameters. *Phil. Trans. R. Soc. Lond. B* **305**, 17–40.
- Ellington, C. P., Van den Berg, C. and Willmott, A. P.** (1996). Leading-edge vortices in insect flight. *Nature* **384**, 626–630.
- Felsenstein, J.** (1985). Phylogenies and the comparative method. *Am. Nat.* **125**, 1–15.
- Fish, F. E.** (1992). Aquatic locomotion. In *Mammalian Energetics: Interdisciplinary Views of Metabolism and Reproduction* (ed. T. E. Tomasi and T. H. Horton), pp. 34–63. Ithaca: Cornell University Press.
- Fish, F. E.** (1993). Influence of hydrodynamic design and propulsive mode on mammalian swimming energetics. *Aust. J. Zool.* **42**, 79–101.
- Fish, F. E.** (1996). Transitions from drag-based to lift-based propulsion in mammalian swimming. *Am. Zool.* **36**, 628–641.
- Fish, F. E., Baudinette, R. V., Frappell, P. B. and Sarre, M. P.** (1997). Energetics of swimming by the platypus *Ornithorhynchus anatinus*: metabolic effort associated with rowing. *J. Exp. Biol.* **200**, 2647–2652.
- Freytmuth, P.** (1988). Propulsive vortical signature of plunging and pitching airfoils. *AIAA J.* **26**, 881–883.
- Fulton, C. J., Bellwood, D. R. and Wainwright, P. C.** (2001). The relationship between swimming ability and habitat use in wrasses (Labridae). *Mar. Biol.* **139**, 25–33.
- Hammer, C.** (1995). Fatigue and exercise tests with fish. *Comp. Biochem. Physiol.* **112A**, 1–20.
- Jensen, M.** (1956). Biology and physics of locust flight. III. The aerodynamics of locust flight. *Phil. Trans. R. Soc. Lond. B* **239**, 511–552.
- Lauder, G. V. and Jayne, B. C.** (1996). Pectoral fin locomotion in fishes: testing drag-based models using three-dimensional kinematics. *Am. Zool.* **36**, 567–581.
- Liu, H., Ellington, C. P., Kawachi, K., Van den Berg, C. and Willmott, A.** (1998). A computational fluid dynamic study of hawkmoth hovering. *J. Exp. Biol.* **201**, 461–477.
- Taylor, E. B. and McPhail, J. D.** (1986). Prolonged and burst swimming in anadromous and freshwater threespine stickleback, *Gasterosteus aculeatus*. *Can. J. Zool.* **64**, 416–420.
- Van den Berg, C. and Ellington, C. P.** (1997). The three-dimensional leading-edge vortex of a ‘hovering’ model hawkmoth. *Phil. Trans. R. Soc. Lond. B* **352**, 329–340.
- Videler, J. J. and Nolet, B. A.** (1990). Costs of swimming measured at optimum speed: Scale effects, differences between swimming styles, taxonomic groups and submerged and surface swimming. *Comp. Biochem. Physiol.* **97A**, 91–99.
- Vogel, S.** (1994). *Life in Moving Fluids*. Second edition. Princeton: Princeton University Press.
- Vogel, S. and LaBarbera, M.** (1978). Simple flow tanks for research and teaching. *BioScience* **28**, 638–643.
- Wainwright, P. C., Bellwood, D. R. and Westneat, M. W.** (2002). Pectoral fin diversity in labrid fishes. *Env. Biol. Fish.* (in press).
- Walker, J. A.** (1998a). Estimating velocities and accelerations of animal locomotion: a simulation experiment comparing numerical differentiation algorithms. *J. Exp. Biol.* **201**, 981–995.
- Walker, J. A.** (1998b). QuickCurve [WWW document] <http://www.usm.maine.edu/bio/faculty/walker.html>: Biological Sciences, University of Southern Maine.
- Walker, J. A.** (1999). Pectoral fin rowing is a drag. *Am. Zool.* **38**, 18A.
- Walker, J. A.** (2002). Functional morphology and virtual models: Physical constraints on the design of oscillating wings, fins, legs and feet at intermediate Reynolds numbers. *Am. Zool.* (in press).
- Walker, J. A. and Westneat, M. W.** (1997). Labriform propulsion in fishes: kinematics of flapping aquatic flight in the bird wrasse *Gomphosus varius* (Labridae). *J. Exp. Biol.* **200**, 1549–1569.
- Walker, J. A. and Westneat, M. W.** (2000). Mechanical performance of aquatic rowing and flying. *Proc. R. Soc. Lond. B* **267**, 1875–1881.
- Weis-Fogh, T.** (1973). Quick estimates of flight fitness in hovering animals, including novel mechanisms for lift production. *J. Exp. Biol.* **59**, 169–230.
- Westneat, M. W.** (1993). Phylogenetic relationships of the tribe Cheilini (Labridae: Perciformes). *Bull. Mar. Sci.* **52**, 351–394.
- Westneat, M. W.** (1997). Phylogenetic relationships of labrid fishes: an analysis of morphological characters. *Am. Zool.* **37**, 198A.
- Whoriskey, F. G. and Wootton, R. J.** (1987). The swimming endurance of threespine sticklebacks, *Gasterosteus aculeatus* L., from the Afon Rheidol, Wales. *J. Fish Biol.* **30**, 335–339.